Int. J. Heat Mass Transfer. Vol. 23, pp. 1127–1136

0017-9310/80/0801-1127 $02.00/0

FORCED CONVECTION HEAT TRANSFER IN HELICALLY RIB-ROUGHENED TUBES

D. L. GEE
Pacific Gas and Electric Co., San Francisco, CA, U.S.A.

and

R. L. WEBB
The Department of Mechanical Engineering, The Pennsylvania State University, University Park, PA 16802, U.S.A.

(*Received* 12 *October* 1979 *and in revised form* 21 *January* 1980)

Abstract—This work presents experimental information for single-phase forced convection in a circular tube containing a two-dimensional rib roughness. It extends the state-of-the-art by examining the effect of the rib helix angle. Although prior studies have proposed that helix angles less than 90° will provide superior heat transfer per unit pumping power, no data have been reported for flow in circular tubes. The present work reports the heat transfer and friction characteristics for air flow with three helix angles (30, 49 and 70°) all having a rib pitch-to-height ratio of 15. The preferred helix angle is approximately 45°. The data are correlated in a form to permit performance prediction with any relative roughness size (e/D). The benefits of the roughness for heat exchanger applications are quantitatively established.

NOMENCLATURE

A, heat transfer surface area;
$B(e^+)$, friction factor correlating parameter for geometrically similar roughness;
$\bar{B}(e^+, \alpha)$, friction factor correlating parameter for helical-rib roughness;
C_p, specific heat;
D, inside diameter of pipe (at base of ribs);
e, rib height;
e^+, roughness Reynolds number, $e^+ = eu^*/\nu = (e/D)Re\sqrt{(f/2)}$;
f, friction factor, $f = \dfrac{\Delta P D}{2L}\dfrac{\rho}{G^2}$;
G, mass velocity (mass flow per unit area);
$g(e^+, Pr)$, heat transfer correlating parameter for geometrically similar roughness;
$\bar{g}(e^+, Pr, \alpha)$, heat transfer correlating parameter for helical-rib roughness;
h, heat-transfer coefficient (smooth tube area basis);
K, overall heat conductance;
L, flow length between pressure taps;
N, number of flow circuits in parallel;
p, distance between ribs;
ΔP, pressure drop;
P, flow friction power;
Pr, Prandtl number;
Q, heat exchange rate, e.g. W;
Re, Reynolds number, $Re = DG/\mu$;
St, Stanton number, $St = h/GC_p$;
u^*, shear velocity $u^* \equiv \sqrt{\tau_0/\rho}$;
U, overall heat-transfer coefficient;
w, width of two-dimensional rib;
x, coordinate distance in flow direction.

Greek symbols

α, helix angle, measured between rib and tube axis;
η, rough-tube efficiency index, $\eta \equiv (St/St_s)/(f/f_s)$;
ν, kinematic viscosity;
ρ, fluid density;
μ, fluid dynamic viscosity;
τ, apparent wall shear stress, $\tau_0 \equiv -\dfrac{D\,dP}{4\,dx}$.

Subscripts

s, refers to smooth tube values;
unsubscripted variables refer to rough surfaces.

INTRODUCTION

THIS WORK is concerned with an improved roughness geometry for application to single-phase fluids in turbulent channel flow. The roughness type considered is internal two-dimensional spiral ribs. Roughness is of interest because it provides a substantial heat-transfer coefficient increase. Used in heat exchangers, internally roughened tubes may be used to reduce surface area, or increase system thermodynamic efficiency via a reduced mean temperature difference for heat exchange.

Because the increased heat transfer coefficient is accompanied by a friction factor increase, the preferred roughness geometry will yield a given heat transfer augmentation with minimum friction increase. The particular roughness type studied in the

present work is a member of a basic type, on which extensive work has been performed. This is 'repeated-rib' roughness, consisting of two-dimensional ribs oriented transverse to the flow, and spaced at a distance p. The dimensionless geometric parameters are e/D, w/e, p/e. The rib helix angle, considered in this study, is an additional geometric variable. Numerous studies have been conducted on transverse-rib roughness (90° helix angle). These studies have encompassed various rib shapes, heights and spacings ($1 < p/e < 40$). The published literature on this roughness are too extensive to survey here. Bergles and Webb's bibliography [1] report 282 studies of roughness with single phase forced convection, many of which treat the transverse-rib roughness. The flow geometries tested include internal internally roughened tubes, parallel-plate flow channels and annuli, in which only the outer surface of the inner tube is roughened.

The previous studies [2, 3] show that the heat-transfer coefficient attains a maximum value for $10 < p/e < 15$, with transverse-rib roughness (90° helix angle). At constant Re, St/St_s attains a maximum as e/D is increased. As Re is increased for this roughness size, the 'efficiency index', $\eta \equiv (St/St_s)/(f/f_s)$ decreases rapidly. Webb and Eckert [4] and Webb [5] present detailed recommendations to select the roughness size (e/D) to yield high St/St_s for arbitrary Re, while maintaining a high efficiency index.

Several investigators have suggested that helical, rather than transverse ribs will yield a given St/St_s with a higher efficiency index. White and Wilkie [20] tested helical-rib roughness applied to the outer surface of a tube in an annular flow configuration. Due to the influence of the smooth outer wall, the friction factor cannot be interpreted for channel flow, in which all bounding surfaces are roughened. They 'transformed' their data using an equivalent diameter concept proposed by Hall [6]. This transformation is intended to remove the smooth wall effect and allow the data to be interpreted for the case of rough bounding walls. The method by which the equivalent diameter is defined has been a controversial subject, and current views are discussed by Dalle Donne and Meyer [7]. White and Wilkie's [20] transformed annulus data showed that decreased helix angle causes St and f to decrease. However, the friction factor decreases faster than the Stanton number. They concluded that the greatest heat-transfer rate per unit pumping power was obtained with $p/e = 8$ at 33° helix angle. Han *et al.* [8] used a parallel-plate channel geometry to study the effect of rib shape, p/e and the rib angle-of-attack. Their data generally supported that of White and Wilkie. Han *et al.* concluded that a 45° angle of attack provided superior performance per unit friction expenditure. Withers' U.S. Patent [9] describes a tube containing internal helical-ribs. Withers argues that superior performance is attained using a rounded rib geometry with $p/e = 15$ and a 39° helix angle.

The technical literature contains no detailed information on the performance of helical-ribs inside circular tubes. This work was undertaken to establish the effect of helical roughness in circular tubes and identify the optimum helix angle.

EXPERIMENTAL PROGRAM

The heat-transfer and friction characteristics of the helical-rib surface geometry were measured for three helix angles ($\alpha = 30$, 49 and 70°). Figure 1 shows the details of the tube geometries. The tubes were made by Noranda Metals, Inc. using a cold swaging process. For each helix angle, a mandrel was machined having grooves corresponding to the helical roughness configuration. The internal roughness was formed by feeding a copper tube lengthwise over the mandrel, while a stationary set of rapidly oscillating rollers located on the periphery of the tube forced copper into the mandrel grooves.

Air was used as the working fluid, encompassing a flow range of $6000 < Re < 65\,000$. In addition to the three rough tubes, a smooth tube geometry was tested to validate the experimental procedure.

Figure 2 is a schematic drawing of the test apparatus. The flow circuit was made from copper tubing and the measuring section was suspended in an insulation filled duct. The test section air flow was supplied by an oilless air compressor. Test section heat was supplied by 25 KVA auto transformer connected to 220 V a.c. power. The measuring section consisted of a 1.52 m long internally roughened hydraulic development section, a 1.52 m long heat-transfer test section and 0.61 m long mixing section, in which a series of baffles were installed. The unheated hydraulic development section and the heat transfer test section had identical internal surface geometries. A 0.22 m^2

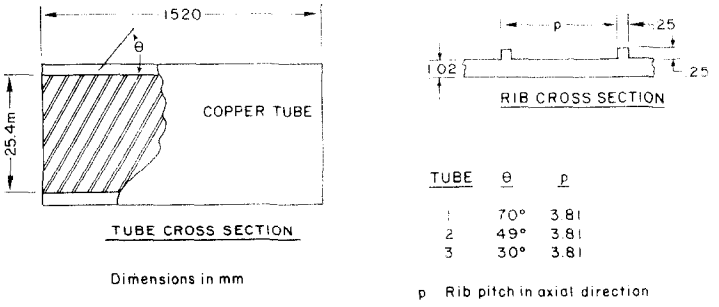

FIG. 1. Helical-rib test sections.

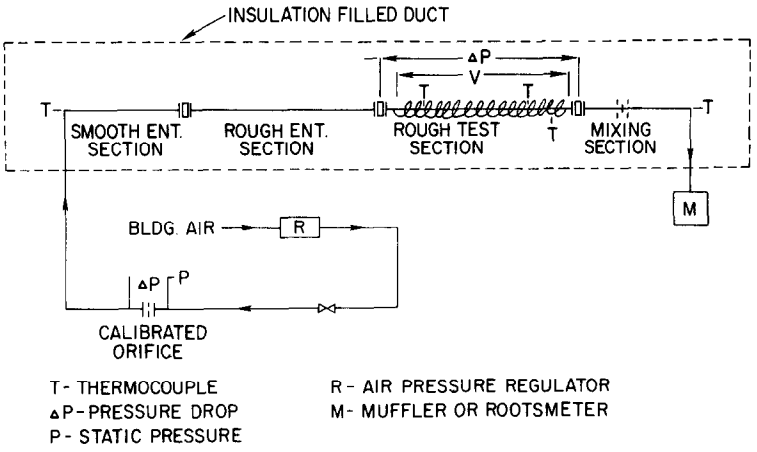

FIG. 2. Schematic drawing of test apparatus.

wood trough, filled with silica aerogel, provided thermal insulation surrounding the entire 4.42 m long measuring section.

The test section was spiral wrapped with 31.75 mm by 0.081 mm Nichrome heating ribbon, with a 0.50 mm spacing between wraps. The Nichrome ribbon was electrically insulated by 0.076 mm thick adhesive-backed Teflon tape cemented to the heating ribbon. The test sections were joined by bolted flanges, between which a 25 mm thick smooth bore Nylon bushing was installed. This bushing contained static pressure taps and provided thermal isolation for the heat transfer test section. The overall distance between pressure taps was 1.55 m. The measured pressure drop was corrected for the 25 mm smooth tube flow length introduced by the Nylon bushings.

Eight thermocouples were installed on each heat transfer tube. The 0.25 mm butt-welded copper–constantan thermocouples were placed in 0.30 mm^2 grooves machined around the circumference of the tube. Thermal contact between the copper tube and the thermocouple junction was assured by peening the copper tube at the junction. Each thermocouple wire was wrapped one-half tube circumference before separation from the tube. The inner surface temperature was obtained by correcting for the temperature drop across the wall. A thermocouple on the outside surface of the heating ribbon facilitated calculation of the test section heat loss.

Air inlet and outlet temperatures were determined by thermocouples positioned at the tube centerline, at the extreme ends of the measuring section. A 0.61 m long baffled mixing section was inserted after the heat transfer test section to insure measurement of the mixed fluid exit temperature.

All thermocouples were constructed of 0.25 mm copper–constantan wire. The reference junctions were provided by a Frigistor electronic ice cell which was periodically checked with a precision thermometer. The temperature-mV conversions were taken from the National Bureau of Standards tables. The thermocouple outputs were measured on a Leeds and Northrup Model 8686 potentiometer.

The volumetric air flow rate was measured with a positive displacement Roots Orifice Prover located at the outlet of the measuring section. For flows beyond the effective range of the Roots meter, a calibrated orifice was used to measure mass flow rate.

The static pressures at the test section and the flow meters were measured by U-tube mercury manometers. The atmospheric pressure was measured using a mercury barometer. Pressure drop across the test section was obtained by a Meriam travelling well micro-manometer. Its accuracy is ± 0.064 mm water.

The electrical power to the test section was determined by measuring the current and voltage supplied to the heating ribbon. The voltage was measured with a Hewlett Packard Model 3466A digital multimeter whose accuracy is $\pm 1.0\%$ of full scale. Current was measured by an a.c. ammeter whose accuracy is $\pm 1.5\%$ of full scale. In addition, the resistance across the section was measured by an impedance bridge and power calculated by $(\text{current})^2 \times$ resistance. In all cases, agreement between the two power measurements was within 1%, thus indicating good experimental accuracy.

The friction factors were determined from pressure drop measurements across the test section without heat input. The friction factors were based on the pressure drop across the 1.52 m test section length, which was preceded by a 1.52 m rough development length.

The heat transfer data were taken following the completion of each set of friction data. In order to reduce temperature measurement errors, heat inputs were selected to provide an air temperature rise of 8–12 K. Steady state was defined by two measurements. First, the variation in wall thermocouples was observed until constant values were attained; then, the outlet air temperature was monitored. Steady state was established if the outlet air temperature did not deviate over a 3-min period.

TEST RESULTS

Before initiating experiments with the rib-roughened surfaces, the friction factor and heat-transfer coefficient were determined for the smooth tube and compared with literature values. The isothermal friction factor and Stanton number results are shown in Figs. 3 and 4 respectively. The solid line on Fig. 3 is the Prandtl–Karman equation [10]. The solid line of Fig. 4 is the Petukhov–Popov [11] equation for turbulent flow in smooth tubes with constant heat flux. The smooth tube data are in good agreement with the accepted correlations.

The rough-tube friction data for 30, 49 and 70° helix angles are shown in Fig. 3. The helix angle (α) is the angle between the rib and the tube axis. The friction factor is approximately 60% higher than the smooth tube at 70° helix angle and decreases as the helix angle decreases. This is shown in Fig. 5 where the friction factor is plotted vs. helix angle.

The rough-tube Stanton number data are shown in Fig. 4. Figure 5 shows the Stanton number vs. helix angle. These figures show the Stanton number decreases as helix angle is decreased. However, further examination of Fig. 5 shows the friction factor decreases at a greater rate than Stanton number. This suggests that the friction contribution due to form drag at large helix angles is greater than the heat transfer due to the flow separation and reattachments. It also suggests the definition of an optimum helix angle, which will give maximum thermal performance per unit friction power.

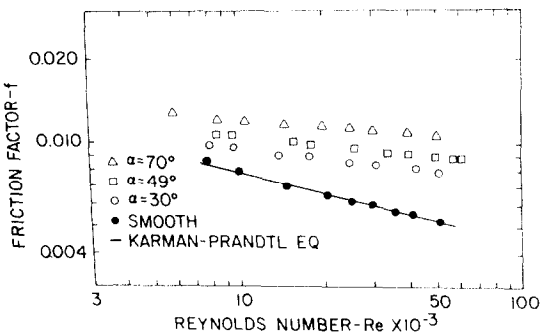

FIG. 3. Friction factor vs. Reynolds number.

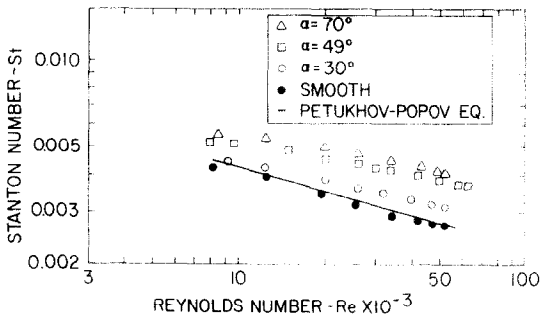

FIG. 4. Stanton number vs. Reynolds number.

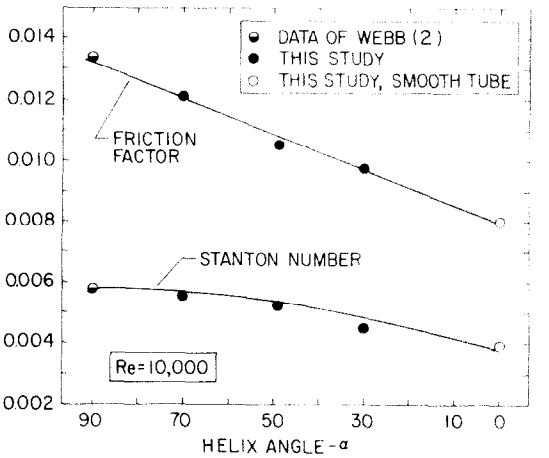

FIG. 5. Stanton number and friction factor vs. helix angle for $Re = 10000$.

CORRELATION OF DATA

The heat transfer and friction data are correlated using accepted correlations for rough tubes. This will permit the data to be interpreted for a wide range of e/D and Re.

Correlations for friction in rough tubes are based on similarity considerations. Two rough surfaces are said to be geometrically similar if their roughness is the same in all respects, except for a single scale factor. For two-dimensional transverse-rib roughness, variation of the helix angle, rib shape or pitch-to-height ratio would constitute geometrically non-similar roughness. Correlation of such data would require empirical corrections to the functions developed on the basis of a similarity law.

Nikuradse [12] used similarity considerations to develop a friction correlation for geometrically similar sand-grain type roughness. He showed excellent correlation of a wide range of roughness sizes using the correlation defined by equation (1).

$$B(e^+) = \sqrt{2/f} + 2.5 \ln (2e/D) + 3.75 \qquad (1)$$

where $e^+ \equiv eu^*/\nu$. For Nikuradse's sand-grain roughnesses, $B(e^+)$ attains a constant value of 8.48 when $e^+ > 70$; this is termed the 'fully rough' regime. Nikuradse's friction similarity law should apply to any geometrically similar roughness type. However $B(e^+)$ will have different values for different roughness types. Webb *et al.* [2] used equation (1), with excellent results, to correlate friction data for turbulent flow in tubes having $p/e = 10$ transverse-rib roughness.

Equation (1) is used to correlate the helical-rib data of the present study. The effect of the helix angle (geometrically non-similar parameter) is accounted for using a power law dependency. The helical-rib data of Fig. 3 are correlated by equation (1), and shown on Fig. 6. The Fig. 6 correlation is represented by equation (2).

$$\bar{B}(e^+, \alpha) = [\sqrt{2/f} + 2.5 \ln(2e/D) + 3.75](\alpha/50)^{0.16} \qquad (2)$$

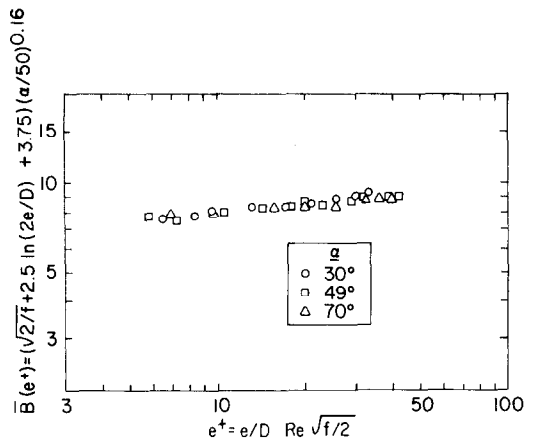

FIG. 6. Correlation of friction data using Nikuradse's Similarity Law [12].

Dipprey and Sabersky [13] developed a heat transfer similarity law, which is complimentary to Nikuradse's friction similarity law. Their model is based on the heat-momentum transfer analogy applied to a two-region flow model. They assume a roughness influenced viscous wall region and a turbulent outer region that is insensitive to roughness. The heat-transfer characteristics of geometrically similar roughness types are accounted for by the friction similarity parameter $B(e^+)$. The data for Pr = constant are correlated in the form of $g(e^+, Pr)$ vs. e^+ where $g(e^+, Pr)$ is defined by equation (3). To account for the Prandtl number dependency, one would use a power law correlation, $g(e^+) \equiv \bar{g}(e^+)Pr^n$

$$g(e^+, Pr) = \frac{f/2st - 1}{\sqrt{f/2}} + B(e^+). \tag{3}$$

Dipprey and Sabersky [13] used equation (3) to correlate their 'sand-grain' roughness data ($0.0024 < e/D < 0.049$, $1.2 < Pr < 5.94$, and Webb *et al.* (2) applied it to $p/e = 10$ transverse-rib roughness ($0.01 < e/D < 0.04$, $0.71 < Pr < 37.6$). The data of both studies were correlated within $\pm 10\%$. The Webb *et al.* study also included tranverse-rib spacings of $p/e = 20$ and 40, which are not geometrically similar to the $p/e = 10$ roughnesses. Using the appropriate $B(e^+)$ for the larger p/e roughnesses, the data for $10 < p/e < 40$ were correlated by equation (3). This result was unexpected, since the different p/e values constitute geometric nonsimilarity.

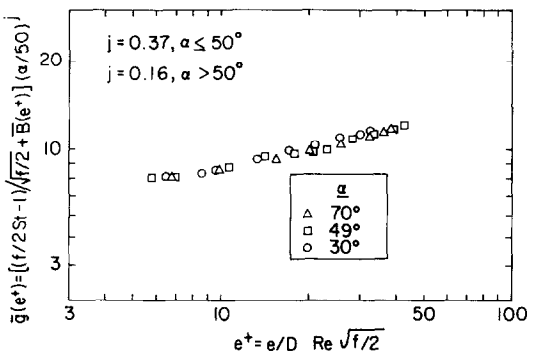

FIG. 7. Correlation of heat-transfer data using Dipprey and Sabersky's Heat Transfer Similarity Law [13].

In the present study, the different helix angles constitute geometrically non-similar roughnesses. Figure 7 shows the Fig. 4 air flow data (Pr = 0.71) correlated using the Dipprey and Sabersky correlation. The Fig. 7 correlation is represented by equation (4), which includes a power law dependency to account for the helix angle. The $\bar{B}(e^+, \alpha)$ is given by equation (2).

$$\bar{g}(e^+, Pr, \alpha) = \left[\frac{f/2St - 1}{\sqrt{f/2}} + \bar{B}(e^+, \alpha)\right]\left(\frac{\alpha}{50}\right)^j \tag{4}$$

where

$$j = 0.37 \quad \text{for } \alpha < 50°$$

$$j = -0.16 \quad \text{for } \alpha > 50°$$

Although different e/D values were not tested in the present study, equations (2) and (4) should predict f and St for arbitrary e/D values, since variation of e/D maintains geometric similarity.

Kader and Yaglom [14] also used a two-region flow model to develop a semi-empirical turbulent heat transfer correlation for two-dimensional roughness. The correlation, for the fully rough flow regime, was developed for two-dimensional roughness in general. Thus, it is applicable to a wide range of roughness shapes, area distributions and heights. Their correlation for air flow is given by equation (5).

$$St = \frac{1.42\sqrt{f/2}}{5(e^+)^{1/4} - 3\ln(e/D) + 5.6 - 4.5/(1 - e/D)^2 + 9.5\sqrt{f/2}}. \tag{5}$$

Figure 8 shows the present results correlated by equation (5). The Kader and Yaglom correlation predicts the helical-rib data quite well.

COMPARISON WITH OTHER STUDIES

The transverse rib study ($\alpha = 90°$) of Webb *et al.* [2] examined a larger Reynolds number (6000–100 000 vs. 6000–65 000), e/D (0.01–0.04 vs. 0.01), and p/e (10–40 vs. 15) range than this investigation. To allow comparison with the present work, the Webb *et al.* air flow data are compared in Fig. 9 with the correlation of this study. Agreement is good, with Webb's data falling slightly below the data of this study for $e^+ > 25$. A first impression suggests that the Webb data yields a higher Stanton number per unit friction. However, examination of η vs. helix angle in Fig. 10 shows that this is not the case.

Figure 11 shows the correlated air data of Han *et al.* [8] who worked with repeated-ribs at different angles of attack in a parallel plate geometry. These data have been corrected using the suggestions of Rehme [15].

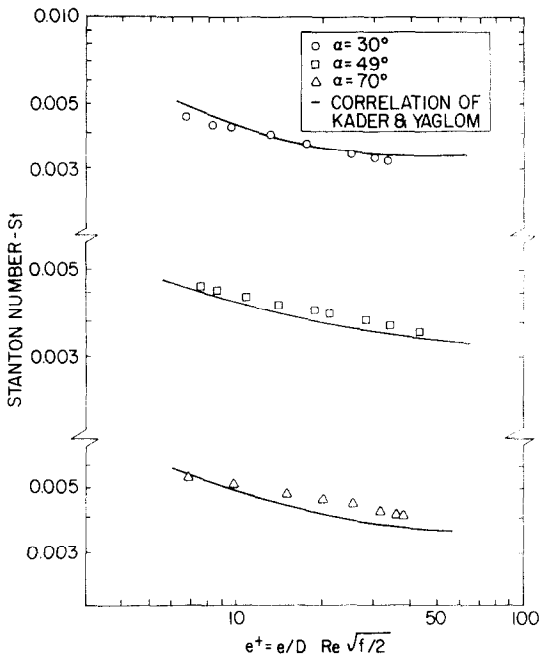

FIG. 8. Correlation of heat-transfer data using Kader and Yaglom correlation [14].

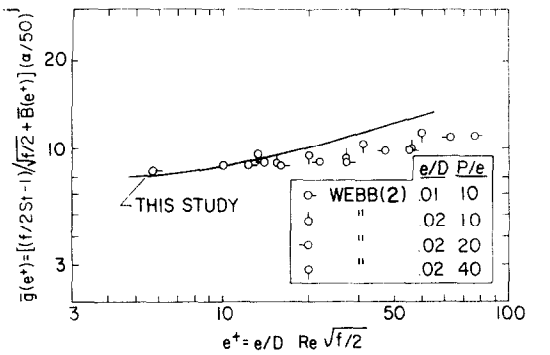

FIG. 9. Comparison of results with transverse-rib data of Webb *et al.* [2].

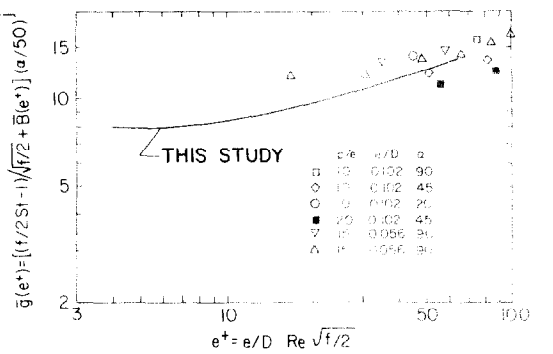

FIG. 11. Comparison of results with repeated-rib data of Han *et al.* [8].

Again, agreement is quite good, with their data more scattered than the results of this study.

Shown in Fig. 12 is the correlated air data of Molloy [16] and Nunner [17], who used transverse-ribs. The rib shapes tested are shown in the table on Fig. 12. Their data are in excellent agreement with the present results. Figure 12 also compares the present results with those reported in Withers' U.S. Patent [9] for air flow in an internal helical-ribbed tube ($e/D = 0.01$, $p/e = 15$ and $\alpha = 39°$). Reference [9] gives data for only one Reynolds number and does not report the Prandtl number for the water flow tests. In a private communication [18], J. Withers stated that their tests were performed with $Pr \simeq 2.8$. We have assumed $\bar{g}(e^+) \propto Pr^{0.57}$ for the Withers data, as reported by Webb *et al.* [2] for transverse-ribs.

Because the Withers data constitutes the only published data on helically-ribbed tubes, it is interesting to compare the Stanton number and friction factors. Both tubes have identical e/D, p/e and α. The Withers tube has a rounded rib vs. the square rib for the present study. The comparison is shown in Table 1. The Table shows the results are nearly identical. It further suggests that the rounded rib shape favored by Withers does not significantly affect the performance.

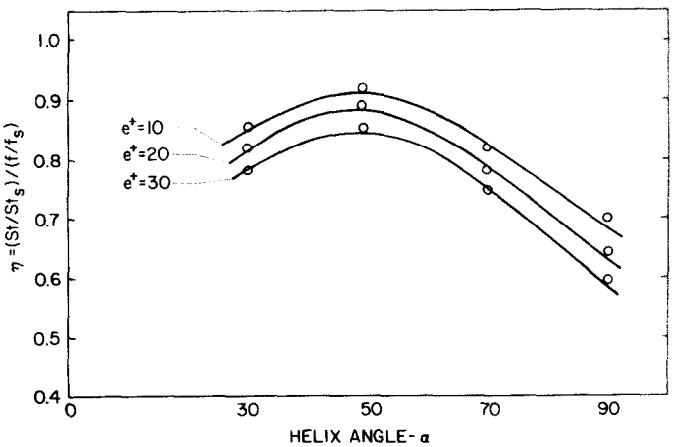

FIG. 10. Efficiency index vs. helix angle.

Table 1. Comparison of Withers' data with the present results

Withers [9]	This study (interpolated for $\alpha = 39°$)
$St = 0.00389$	$St = 0.00392$
$f = 0.00850$	$f = 0.00890$
$SSt/f = 0.91$	$2St/f = 0.88$

For $Re = 35\,000$ and $Pr = 0.71$ ($e/D = 0.01$, $p/e = 15$ and $\alpha = 39°$).

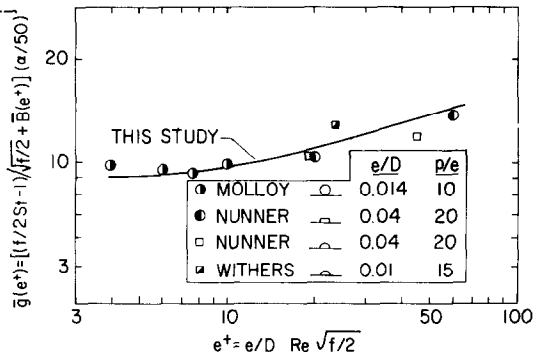

FIG. 12. Comparison of results with Molloy [16], Nunner [17] and Withers [9].

APPLICATION TO HEAT EXCHANGERS

A given roughness will not yield a uniformly high efficiency index when operated over a wide Reynolds number range. This is illustrated in Fig. 14 which shows η vs. e^+, which is drawn with $Re = Re_s$. This figure shows that η decreases with increasing roughness Reynolds number (e^+). Conversely, Fig. 13 shows that St/St_s increases with increasing e^+, and starts to level-off at $e^+ \simeq 20$. These considerations suggest that the preferred operating condition is approximately $e^+ = 20$. Figure 10 and 14 clearly show that the maximum η is obtained with the 49° helix angle. Operated at $e^+ = 20$, the 49° helix angle tube gives $St/St_s = 1.4$ with $\eta = 0.90$.

The friction and heat transfer correlations are valid for geometrically similar roughnesses. Therefore, the present results for $e/D = 0.01$ may be interpreted for other e/D values at constant p/e and α. Assume a design requires operation at $Re = 62\,500$. Using the recommended design condition $e^+ = 20$, we may calculate the required e/D. For $\alpha = 49°$ at $e^+ = 20$, $B(e^+) = 8.55$ and $e^+ = 20 = (e/D)Re\sqrt{f/2}$. Using these values in equation (1), we obtain $e/D = 0.005$. This example clearly shows the preferred roughness size varies with Reynolds number.

Webb and Eckert [4] discuss three basic heat exchanger applications for internally rough surfaces. The design objectives are stated relative to a heat exchanger having smooth inner tube surfaces operating at fixed total flow rate and entering fluid conditions. The three design objectives are:

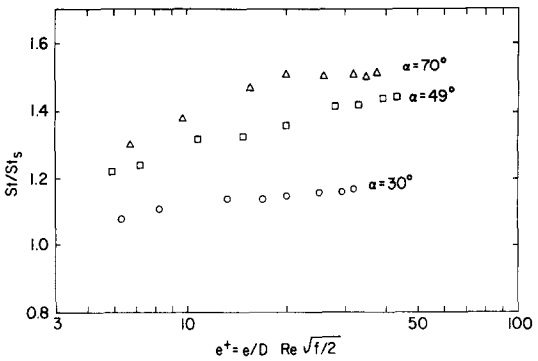

FIG. 13. St/St_s vs. e^+.

1. Reduced tube material for equal pumping power and heat duty ($P/P_s = Q/Q_s = 1$).
2. Increased UA for equal pumping power and heat exchange surface area ($P/P_s = A/A_s = 1$). A higher UA may be used to obtain increased heat duty or to secure reduced mean temperature difference.
3. Reduced pumping power for equal heat duty and surface area ($Q/Q_s = A/A_s = 1$).

The design advantage offered by helical-rib tubing will be calculated for each design objective, assuming fixed tube diameter and prescribed wall temperature (all of the thermal resistance is on the tube side).

The relative heat conductance ($K/K_s \equiv hA/h_sA_s$) of the rough and smooth tube exchangers is

$$\frac{K}{K_s} = \frac{St}{St_s} \cdot \frac{A}{A_s} \cdot \frac{G}{G_s}. \tag{6}$$

The corresponding friction power ratio is

$$\frac{P}{P_s} = \frac{f}{f_s} \frac{A}{A_s} \left(\frac{G}{G_s}\right)^3. \tag{7}$$

It may be necessary to operate the rough tube at a lower velocity than the smooth tube to obtain equal friction power. This may be accomplished by increasing the number of rough tubes in parallel (N) since $N/N_s = G_s/G$. Eliminating G/G_s from equations (6) and (7) gives

$$\frac{K/K_s}{(P/P_s)^{1/3}(A/A_s)^{2/3}} = \frac{St/St_s}{(f/f_s)^{1/3}}. \tag{8}$$

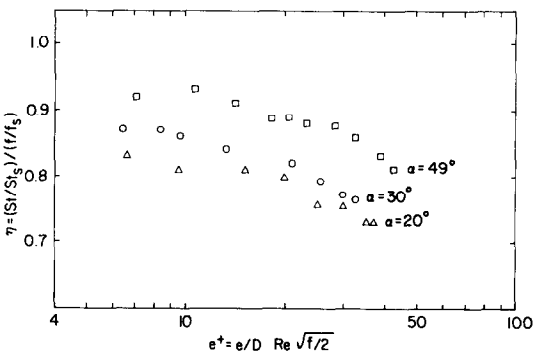

FIG. 14. Efficiency index (η) vs. e^+.

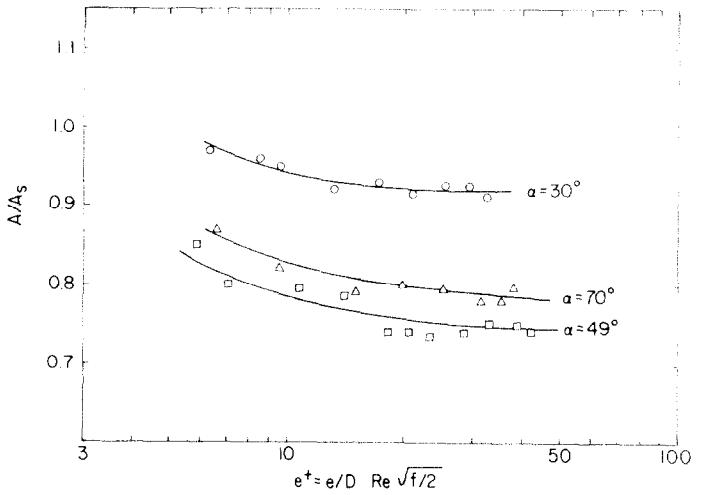

FIG. 15. A/A_s vs. e^+.

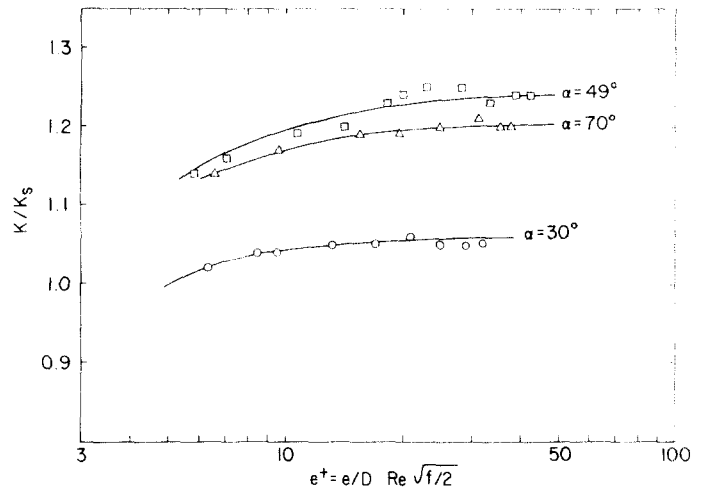

FIG. 16. K/K_s vs. e^+.

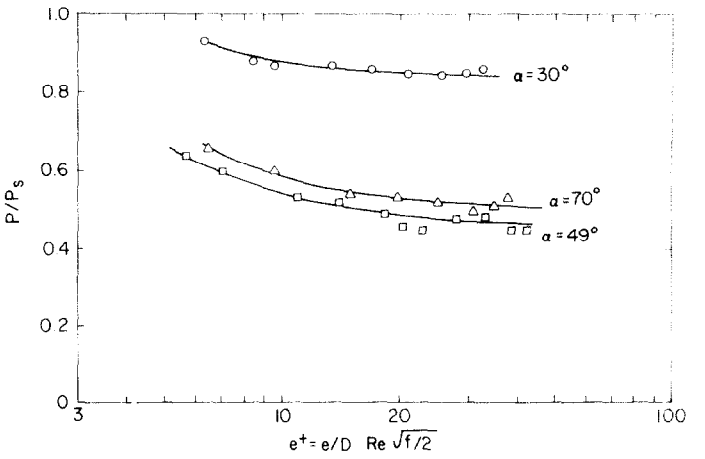

FIG. 17. P/P_s vs. e^+.

Equation (8) provides an expression containing the parameters K/K_s, P/P_s, and A/A_s defined in terms of f/f_s and St/St_s. Two of these parameters are set equal to the value 1.0 and the remaining parameter is expressed in terms of a Stanton-friction factor ratio. Figure 15 shows A/A_s vs. e^+ for the data of this study, and Figs. 16 and 17 for K/K_s and P/P_s, respectively. The 49° helical ribs provide the highest performance. At the recommended operating condition of $e^+ = 20$, the 49° helix angle will:

1. Reduce heat exchange surface area by approximately 25%.
2. Increase heat conductance by approximately 27%.
3. Reduce pumping power by approximately 50%.

Bergles *et al.* [19] developed similar performance evaluation criteria for enhanced heat-transfer surfaces. However, several of their proposed performance criteria involve a reduction of rough-tube mass flow rate. It is difficult to obtain a significant performance improvement if the exchanger flow rate is reduced. This is because the exchanger must operate at a greater thermal effectiveness. Hence, the rough tube must provide additional hA to compensate for the increased thermal effectiveness.

CONCLUSIONS

1. This study clearly establishes that helical rib-roughness yields greater heat transfer per unit friction than transverse rib-roughness. The preferred helix angle is approximately 49°.
2. The data are correlated using models previously developed by Nikuradse, and Dipprey and Sabersky. The Kader and Yaglom correlation also provides good results.
3. Analysis of the correlated results establishes a preferred operating condition of $e^+ \simeq 20$. This provides high heat-transfer performance with minimum friction penalty.
4. Performance evaluation criteria are employed to demonstrate the performance benefits offered for three heat exchanger applications..

Acknowledgement—This work was funded under a research initiation grant from The Pennsylvania State University. The support of Mr T. C. Carnavos in providing the helical-ribbed tubes is greatly appreciated.

REFERENCES

1. A. E. Bergles and R. L. Webb, Bibliography on augmentation of convective heat and mass transfer, *Previews Heat Mass Transfer* **4**, No. 4, 89–106 (1978).
2. R. L. Webb, E. R. G. Eckert and R. J. Goldstein, Heat transfer and friction in tubes with repeated-rib roughness, *Int. J. Heat Mass Transfer* **14**, 601–617 (1971).
3. N. Sheriff and P. Gumley, Heat transfer and friction properties of surfaces with discrete roughness, *Int. J. Heat Mass Transfer* **9**, 1297–1320 (1966).
4. R. L. Webb and E. R. G. Eckert, Application of rough surfaces to heat exchanger design, *Int. J. Heat Mass Transfer* **15**, 1647–1658 (1972).
5. R. L. Webb, Toward a common understanding of the performance and selection of roughness for forced convection, in *Studies in Heat Transfer: A Festschrift for E.R.G. Eckert*, Ed., T. Irvine *et al.*, pp. 247–252. Hemisphere, Washington, D.C. (1979).
6. W. B. Hall, Heat transfer in channels having rough and smooth surfaces, *J. Mech. Engng Sci.* **4**, 287–291 (1962).
7. M. Dalle Donne and L. Meyer, Turbulent convective heat transfer from rough surfaces with two-dimensional rectangular ribs, *Int. J. Heat Mass Transfer* **20**, 583–620 (1977).
8. J. C. Han, L. R. Glicksman and W. M. Rohsenow, An investigation of heat transfer and friction for rib-roughened surfaces, *Int. J. Heat Mass Transfer* **21**, 1143–1156 (1978).
9. J. G. Withers, Heat transfer tube having multiple internal ridges, U.S. Patent 3, 779, 312 (1973).
10. J. O. Hinze, *Turbulence*, 2nd ed., p. 722. McGraw-Hill, New York (1975).
11. B. V. Karlekar and R. M. Desmond, *Engineering Heat Transfer*, p. 350, West, St. Paul (1977).
12. H. Schlicting, *Boundary Layer Theory*, 6th ed., p. 578, McGraw-Hill, New York.
13. D. F. Dipprey and R. H. Sabersky, Heat and momentum transfer in smooth and rough tubes, *Int. J. Heat Mass Transfer* **6**, 329–353 (1963).
14. B. A. Kader and A. M. Yaglom, Turbulent heat and mass transfer from a wall with parallel roughness ridges, *Int. J. Heat Mass Transfer* **20**, 345–358 (1977).
15. K. Rehme, Comments on: An investigation of heat transfer and friction for rib-roughened surfaces, *Int. J. Heat Mass Transfer* **22**, 491–492 (1979).
16. J. Molloy, Rough tube friction factors and heat transfer coefficients in laminar transition flow, AERE Report R-5415 (1967).
17. W. Nunner, Heat transfer and pressure drop in rough pipes, *VDI-Forsch* **22**, 4558 (1959). Eng. trans., *AERE Lib. Trans.* 786 (1958).
18. J. G. Withers, Private communication with R. L. Webb (June 1979).
19. A. E. Bergles, A. R. Blumenkrantz and J. Taborek, Survey and evaluation of techniques to augment convective heat transfer, *Proc. 13th Nat. Heat Trans. Conference*, Paper 9, AIChE, New York (1972).
20. L. White and D. Wilkie, The heat transfer and pressure loss characteristics of some multi-start ribbed surfaces, *Augmentation of Convective Heat and Mass Transfer*, A. E. Bergles and R. L. Webb, eds, pp. 55–62, ASME, New York (1970).

CONVECTION THERMIQUE FORCEE DANS DES TUBES RUGUEUX AVEC ARETE HELICOIDALE

Résumé—On présente une étude expérimentale sur la convection forcée monophasique dans un tube circulaire contenant une rugosité bidimensionnelle. C'est une mise au point sur l'effet de l'angle de l'arête hélicoïdale. Bien que des études aient proposé que des angles de l'hélice inférieurs à 90° donnent un meilleur transfert de chaleur vis-à-vis de la puissance de pompage, aucun résultat n'a été fourni pour les écoulements dans les tubes circulaires. On donne ici les caractéristiques du transfert thermique et du frottement pour un écoulement d'air avec trois angles d'hélice (30,49 et 70°), avec pour tous un rapport pas- hauteur de 15. L'angle d'hélice préféré est approximativement 45°. Les données sont présentées de façon à permettre une prédiction de performance avec une rugosité relative (e/D) quelconque. Les bénéfices de la rugosité pour des applications aux échangeurs de chaleur sont quantitativement établis.

WÄRMEÜBERTRAGUNG DURCH ERZWUNGENE KONVEKTION IN SPIRALRIPPENFÖRMIG AUFGERAUHTEN ROHREN

Zusammenfassung—Diese Arbeit liefert experimentelle Informationen über einphasige erzwungene Konvektion in einem Kreisrohr, das mit zweidimensionaler Rippenrauhigkeit versehen ist. Sie erweitert den derzeitigen Wissensstand um die Untersuchung des Einflusses der Steigung der Rippenspirale. Obwohl aus früheren Untersuchungen bekannt ist, daß Spiralwinkel von weniger als 90° besseren Wärmeübergang pro Einheit der Pumpenleistung bewirken, ist über keine Versuchsergebnisse für die Strömung in Kreisrohren berichtet worden. In der vorliegenden Arbeit werden für Luftströmung mit drei Spiralwinkeln (30, 49 und 70°), bei denen das Teilungs–Höhenverhältnis jeweils 15 war, die Wärmeübergangs- und Reibungscharakteristiken angegeben. Der bevorzugte Steigungswinkel ist angenähert 45°. Die Daten sind in einer Form korreliert worden, die Leistungsberechnungen bei beliebigen relativen Rauhigkeitsgrößen (e/D) ermöglicht. Die Vorteile der Rauhigkeit für die Anwendung in Wärmeübertragern werden quantitative bestimmt.

ТЕПЛОПЕРЕНОС ВЫНУЖДЕННОЙ КОНВЕКЦИЕЙ В ТРУБАХ СО СПИРАЛЬНО-РЕБРИСТОЙ ШЕРОХОВАТОСТЬЮ

Аннотация — Проведено экспериментальное исследование однофазной вынужденной конвекции в круглой трубе с двухмерной ребристой шероховатостью. По сравнению с ранее проводившимися исследованиями учитывалось влияние угла наклона ребра спирали. Хотя в прежних работах отмечалось, что при углах наклона, меньших 90°, получаются более высокие значения величины теплового потока на единицу мощности, затрачиваемой на прокачку, однако эти исследования не касались течения в круглых трубах. В данной работе представлены данные по теплообмену и трению при течении воздуха в трубах с тремя углами наклона ребра спирали (30, 49 и 70°) при отношении шага ребра к высоте, равном 15. Наиболее оптимальным является угол в 45°. Результаты обобщены таким образом, чтобы рабочие характеристики могли быть определены при любом значении относительной шероховатости (e/D). Дана количественная оценка влияния шероховатости поверхностей теплообменников.